Antimicrobial Carbon Nanodots: Photodynamic Inactivation and Dark Antimicrobial Effects on Bacteria by Brominated Carbon Nanodots

Rachael Knoblauch, Amanda Harvey, Estelle Ra, Ken M. Greenberg,

*Judy Lau, Elizabeth Hawkins, and Chris D. Geddes**

Institute of Fluorescence and Department of Chemistry and Biochemistry, University of Maryland Baltimore County, 701 East Pratt Street, Baltimore, Maryland 21202, USA

*all correspondence: geddes@umbc.edu

KEYWORDS: photodynamic inactivation, carbon nanodots, heavy atom effect, photosensitization, reactive oxygen species, reactive nitrogen species, antibiotic resistance, phosphorescence

Electronic Supplementary Information (ESI)

APPENDIX A:

CALCULATING HIGH DENSITY ESTIMATES OF COLONY FORMATION IN ANTIMICROBIAL EXPERIMENTS

In order to perform quantitative assessment of bacterial colony growth and subsequent calculations, it was sometimes necessary to estimate colony counts in the case of high-density growth. To achieve this, the Colony Counter plug in for ImageJ was used. The low-density method is shown in Figure A1a.

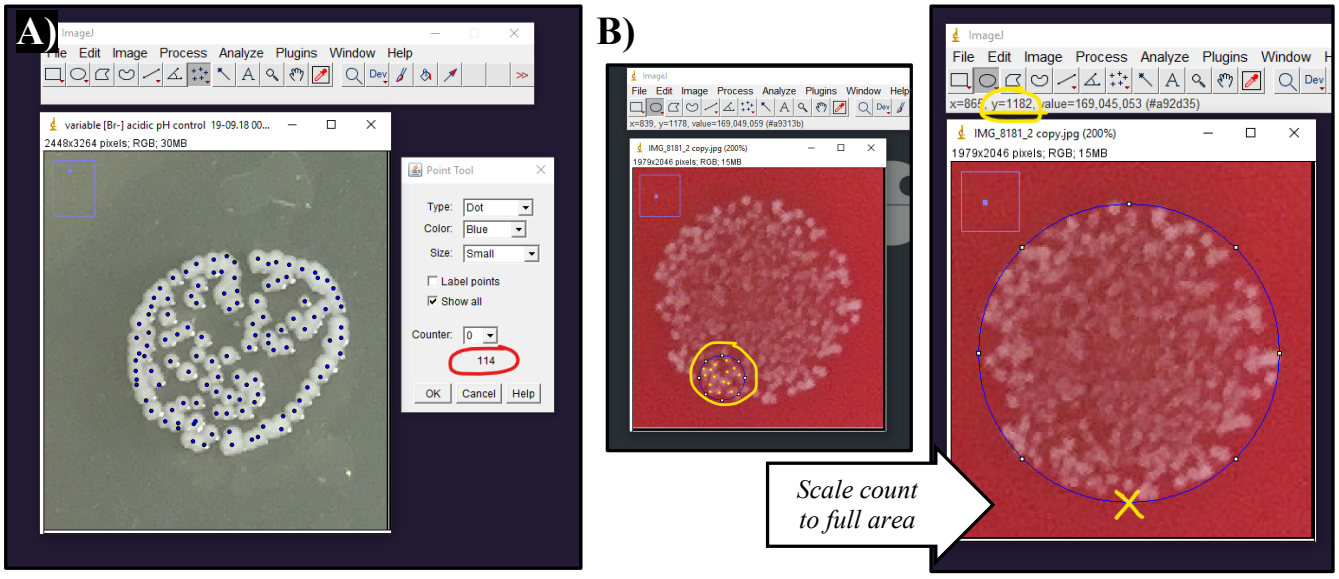

Figure A1. Procedure for obtaining a high density estimate for colony counting using ImageJ. *A)* Screen capture of low-density colony counting using the multi-point tool. *B)* Screen capture for high density estimate using the circle selection and multi-point tool.

When discrete colonies were not observed, estimates were obtained by isolating a circular area within the overall sample size that demonstrated countable colonies (Fig. A1b, left). Colonies were counted using the multi-point tool, and the area determined using the calculated pixel diameter from ImageJ coordinates. The entire surface was then selected, and the area calculated (Fig. A1b, right). The ratio of areas was then used to scale the discrete colony counts to the entire selection, as shown in Equation A1.

$$Counts_{Total} = Counts_{Selection} * \frac{Area_{Total}}{Area_{Selection}} \qquad \text{(Equation A1)}$$

To reduce bias, estimates were calculated independently by n = 3 individuals and averaged.

APPENDIX B:
CHARACTERIZATION OF BROMINATED CARBON NANODOTS

Characterization of brominated carbon nanodots (BrCND) follows data previously reported in a 2018 study by our laboratory.[B1] These data are pertinent to this publication and are summarized within this appendix. For all cited data, the reader is referred to Ref. [B1] for experimental details. Concerning triplet character of the carbon dots, bromination is a key parameter to observe phosphorescence ($T_1 \rightarrow S_0$) from these structures. This is illustrated in Figure B1, in which emissions from carbon dots collected into water ("Water Dots") are compared to those collected into hydrobromic acid ("Br Dots" / "BrCND") both under steady state (Fig. B1a) and off-gated parameters (Fig. B1b).

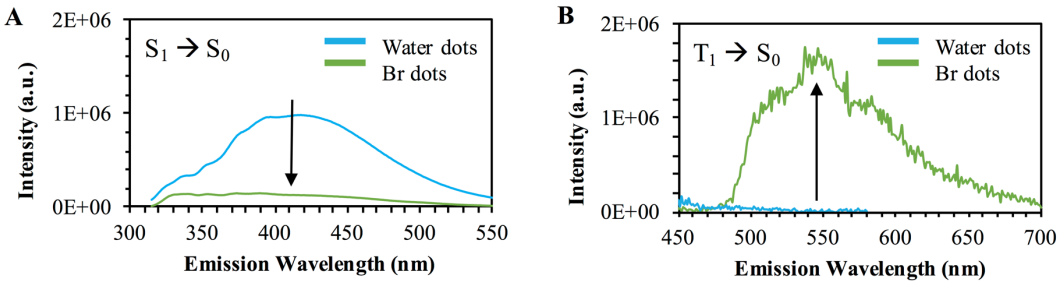

Figure B1. Luminescence emission profiles of carbon nanodot structures collected for 4 hours, suspended in glycerol, and excited at 300 nm. *A)* Steady-state collection of fluorescence emission from carbon dots directly collected into deionized water ("Water dots") and 5M hydrobromic acid ("Br dots"). *B)* Off-gated detection of phosphorescence emission from water and Br dots. Reproduced from Ref. [B1] with permission from the PCCP Owner Societies.

Relative to water dots, the BrCND have reduced fluorescence ($S_1 \rightarrow S_0$) emission (Fig. B1a); this is expected with increased incidence of intersystem crossing, as higher occupation of and emission from excited triplet states reduces the overall probability of emission from singlet excited states. Further, this decrease is accompanied by the long-lived signal emerging at ~550 nm (Fig. B1b), which is not detected for the water dots alone. This confirms that the heavy atom effect is essential in the observation of triplet character from the carbon nanodot structures described herein.

It is interesting to note, however, that the heavy atom effect may be employed both in an *internal* or *external* regime, in which the bromine atoms are located within the carbon dot structure or within the solvent respectively. To confirm that the bromide ions do in fact molecularly modify the carbon dot structures during collection, BrCND were collected directly into HBr at varying burn times (Fig. B2a).

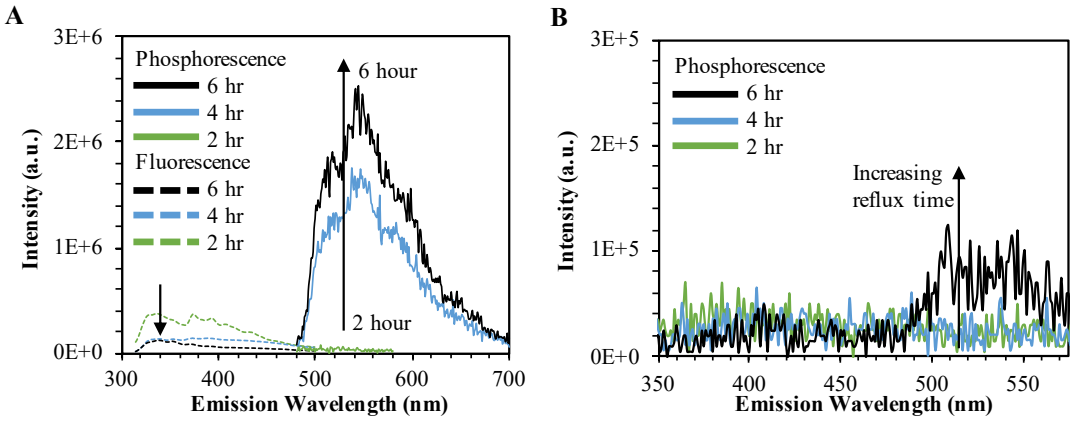

Figure B2. Luminescence emission profiles of carbon nanodot structures collected for various time intervals, suspended in glycerol, and excited at 300 nm. *A)* Phosphorescence (solid lines) and fluorescence (dashed lines) from brominated carbon nanodots of 2, 4, and 6-hour burn times with direct hydrobromic acid collection. *B)* Phosphorescence spectra of carbon dots first collected into water, then refluxed with hydrobromic acid, for 2, 4, and 6-hour periods. Reproduced from Ref. [B1] with permission from the PCCP Owner Societies.

The phosphorescence of these structures increases with time, owing to increased bromine dot concentrations. Conversely, carbon dots were first collected into water and were then refluxed with HBr for various time intervals (Fig. B2b). It should be noted that only at lengthy reflux times were any, and in fact quite weak, phosphorescent signals detected. This indicates that the heavy atom effect occurs for these structures in an internal regime and is therefore not significantly impacted by dissolved bromide ions.

The absorption spectra for the BrCND structures are shown in Figure B3a for solutions analyzed immediately after collection, 12 days post-collection, and 3 weeks post-collection. For these studies, ambient storage conditions included temperatures of ~20°C and light exposure from both fluorescent

laboratory lighting and sunlight from laboratory windows. Photographs of corresponding solutions are provided in Figure B3b.

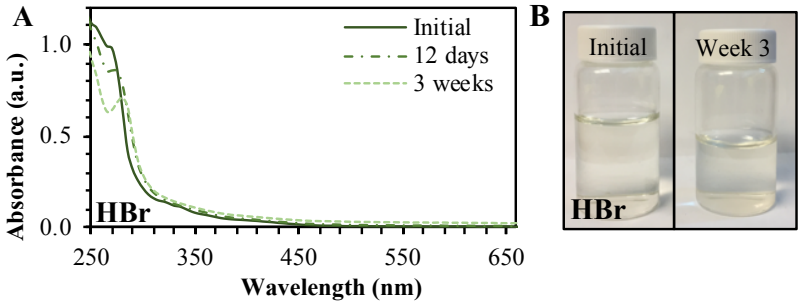

Figure B3. Relative stability of carbon dots directly collected into 5M HBr (brominated carbon nanodots, labeled "HBr" here) for a 4 hour time period. *A)* Absorption spectra of the bromine dots, measured at 0 (Initial), 12-day, and 3-week time spans of general lab storage. *B)* Real-color photographs of samples under room light both at 0 (*left*) and 3-week (*right*) time spans. Please note that the volume decreased due to use of the sample for other experiments, not due to evaporation in storage conditions. Adapted from Ref. [B1] with permission from the PCCP Owner Societies.

Fluorescence lifetime analysis was also performed for BrCND structures with varying pH (Fig. B4).

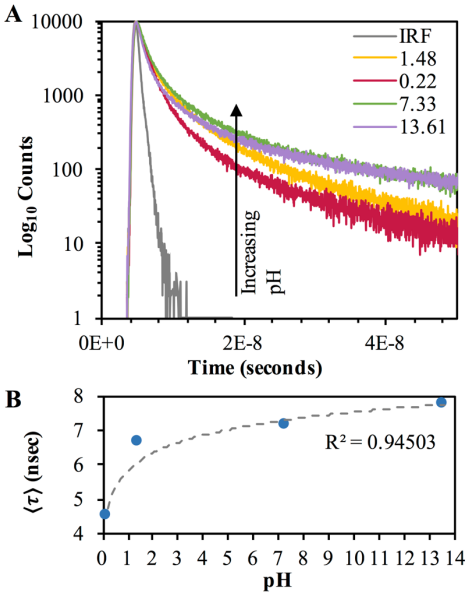

Figure B4. Decay of fluorescence emission from 4-hour brominated carbon nanodots (in glycerol) in varying pH environments, monitored using time correlated single photon counting techniques (λ_{ex} = 311 nm, λ_{em} > 350 nm). *A)* Decay profiles of each sample. *B)* Amplitude weighted lifetimes ($\langle\tau\rangle$) calculated from (A) plotted as a function of solution pH. Reproduced from Ref. [B1] with permission from the PCCP Owner Societies.

Our previous report found that phosphorescence detection was pH-dependent, with a roughly on→off and off→on response noted for fluorescence and phosphorescence respectively as the pH was cycled from basic/neutral to acidic conditions.[B1] Fluorescence lifetime increases with pH for these structures, likely owing to reduced quenching of the singlet excited states by intersystem crossing in non-phosphorescent conditions. Tabulated lifetime values can be found in Reference [B1].

Finally, to better characterize these structures for this study we performed zeta potential, gel electrophoresis, and dynamic light scattering (DLS) measurements as discussed in the main text (Fig. B5).

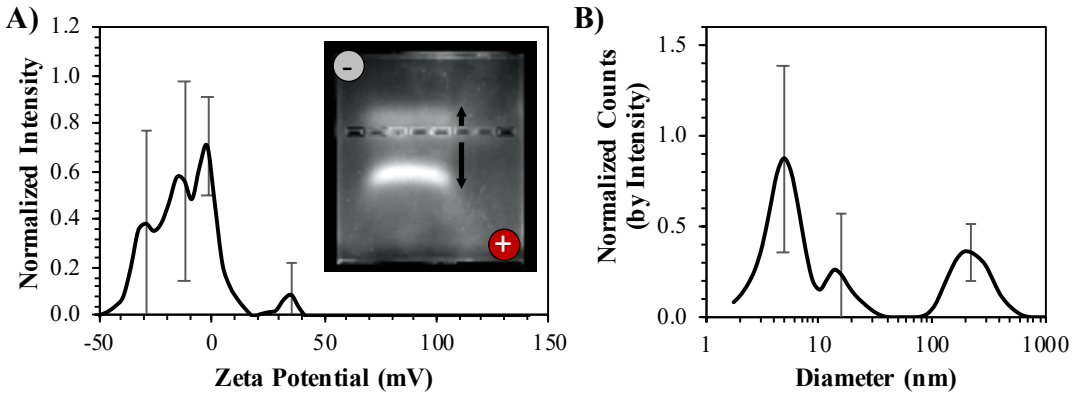

Figure B5. Physical properties of brominated carbon nanodots (BrCND). *A)* Spectrum of normalized Zeta potential measurements for BrCND at pH = 3.5 (μM additional salt concentrations). **Inset.** Gel electrophoresis (1.75% agarose gel, 100V, 40 min) of BrCND samples demonstrating charge distribution of species. *B)* Size analysis of acidic BrCND using dynamic light scattering, reported as normalized counts by intensity. Both spectra are the average of n = 3 sequential measurements; error is from standard deviation.

Regarding surface charge, it was found from the zeta potential and electrophoresis measurements that the bromine dot solution contained a mixture of negative and positively charged species (Fig. B5a). DLS measurements also revealed a degree of polydispersity, with reported particle sizes of ~5 and ~11 nm, as well as larger aggregate particles of ~200 nm diameter.

[B1] Knoblauch, R.; Bui, B.; Raza, A.; Geddes, C. D., Heavy carbon nanodots: a new phosphorescent carbon nanostructure. *Physical Chemistry Chemical Physics*, **2018**, *20*(22), 15518-15527. https://doi.org/10.1039/C8CP02675K.

APPENDIX C:
SUPPLEMENTARY FIGURES

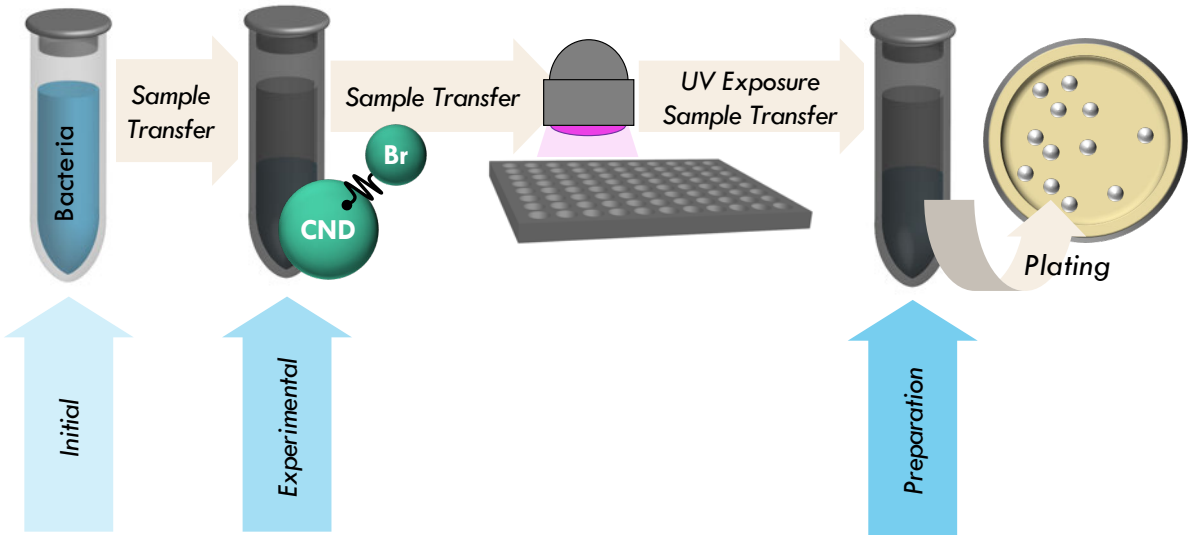

Scheme S1. Experimental schematic for the bacterial experiment design used to assess the antimicrobial efficacy of brominated carbon nanodots (BrCND) under varying exposure conditions.

Appendix C: Supplementary Figures

Experiment	Experimental Solution Solvent	Figure #
Time dependence of photosensitization	1) Deionized water 2/3) pH 3.2 ± 0.2, [Br-] = 0.4M, [Na_3Cit] = ~0.16M 4/5) pH 3.2 ± 0.2, BrCND, [Br-]$_{max}$ = 0.4M, [Na_3Cit] = ~0.16M	4, S6
UV exposure effects (Control)	All solvents = deionized water	S7/9/11 (A)
Range of pH effects (Control)	HBr diluted to achieve desired pH (2-6) Deionized water	S7/9/11 (B)
Concentration of bromide effects (Control)	Sodium bromide in deionized water	S7/9/11 (C)
[Br-] at pH 3.5 (Control)	pH 3.5, [Na_3Cit] = 0.179 ± 0.001 M, variable [Br-] pH 3.5, [Na_3Cit] = 0.18 M, [NO_3^-] = 0.300M Deionized water	S8/10/12
Photosensitization using UV and white light	Deionized water pH 3.5, BrCND, [Br-]$_{max}$ = 0.4M, [Na_3Cit] = ~0.16M pH 3.5, [Na_3Cit] = 0.179 ± 0.001 M, variable [Br-]	5
Concentration (BrCND) dependence of photosensitization	*Staphylococcus aureus* pH 3.0, BrCND, [Br-]$_{max}$ = 0.37 ± 0.01 M, [Na_3Cit] = 0.158 ± 0.003 M pH 3.0, [Br-] = 0.367 M, [Na_3Cit] = 0.154 M — *Escherichia coli* pH 3.0, BrCND, [Br-]$_{max}$ = 0.372 ± 0.006 M, [Na_3Cit] = 0.166 ± 0.001 M pH 3.0, [Br-] = 0.367 M, [Na_3Cit] = 0.154 M	6-7, S13 — 7-8 S15/18
Photosensitization effects for CND (Control)	pH 3.0, CND, [Br-] = 0.36 ± 0.03 M, [Na_3Cit] = 0.155 ± 0.003 M pH 3.0, [Br-] = 0.367 M, [Na_3Cit] = 0.154 M	7 S14/16

Table S1. Experimental Solvents Used for the Antimicrobial Efficacy of Brominated Carbon Nanodot Bacterial Experiments and Controls.

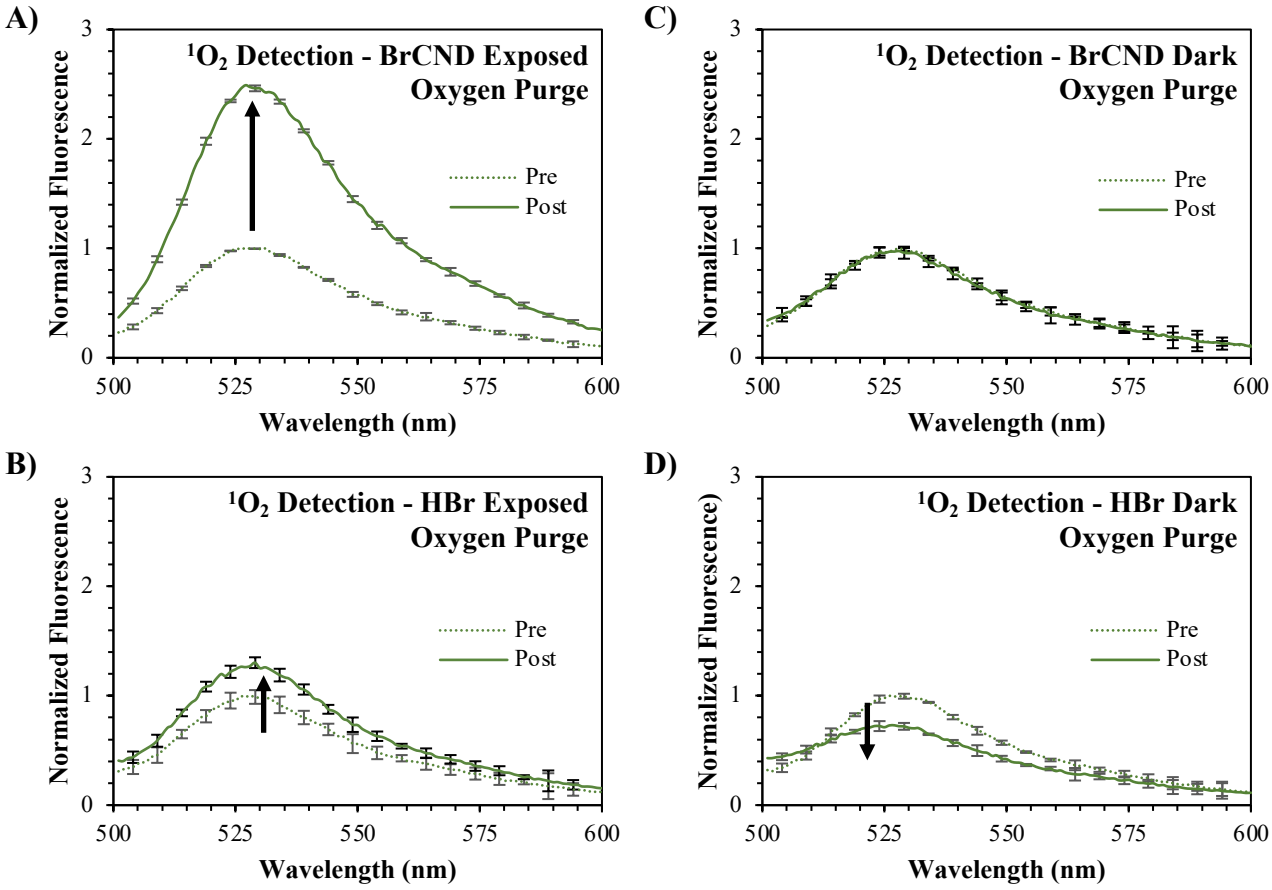

Figure S1. Normalized fluorescence spectra of Singlet Oxygen Sensor Green ("SOSG," $\lambda_{excitation}$ = 473 nm) before ("pre," maximum intensity = 1) and after ("post") exposure with brominated carbon nanodots ("BrCND," pH = 3.0, $\lambda_{exposure}$ = 365 nm, ~0.5 J•cm^{-2}) under oxygen-purged conditions. Fluorescence spectra are reported for SOSG UV-exposed with *A)* BrCND and *B)* hydrobromic acid ("HBr," pH = 3.0) control, and under dark conditions (no exposure) for *C)* BrCND and *D)* HBr control solution. Reported spectra are the average of three analyzed solutions from one sample trial.

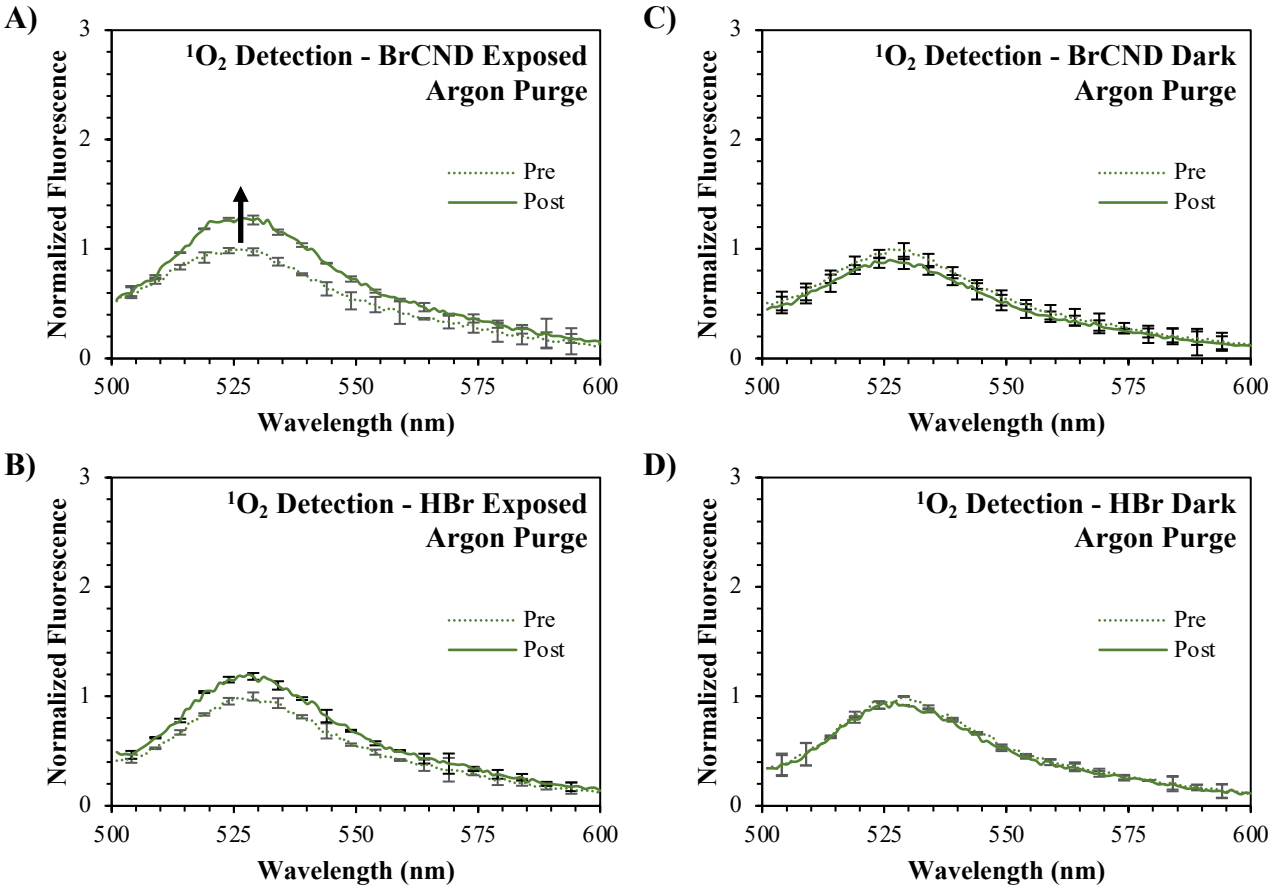

Figure S2. Normalized fluorescence spectra of Singlet Oxygen Sensor Green ("SOSG," $\lambda_{excitation}$ = 473 nm) before ("pre," maximum intensity = 1) and after ("post") exposure with brominated carbon nanodots ("BrCND," pH = 3.0, $\lambda_{exposure}$ = 365 nm, ~0.5 J•cm^{-2}) under argon-purged conditions. Fluorescence spectra are reported for SOSG UV-exposed with *A)* BrCND and *B)* hydrobromic acid ("HBr," pH = 3.0) control, and under dark conditions (no exposure) for *C)* BrCND and *D)* HBr control solution. *B/C)* Reported spectra are the average of three analyzed solutions from one sample trial. *A/D)* Spectra are the average of two solutions from one sample trial.

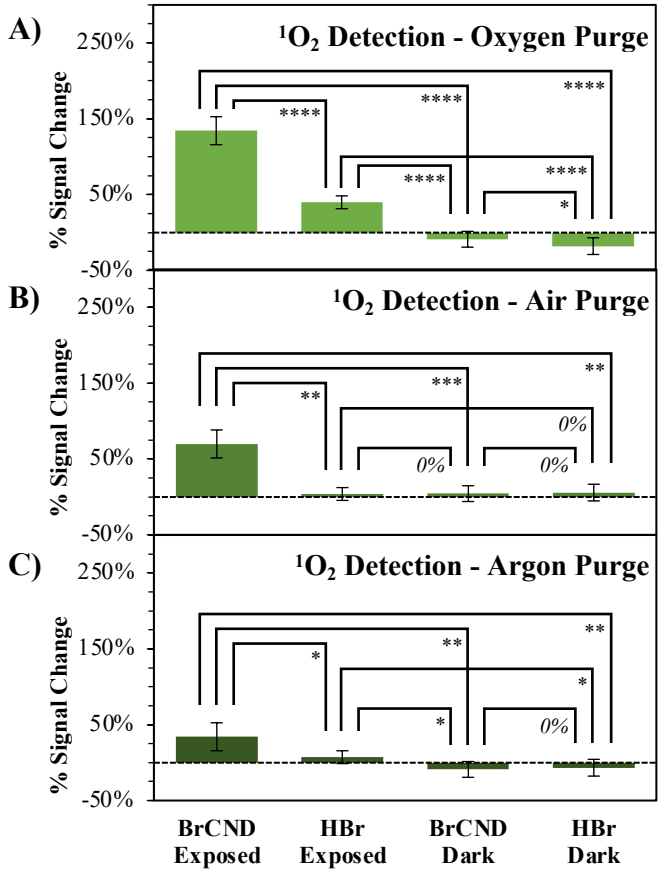

Figure S3. Statistical analysis of percent signal change values determined for singlet oxygen generation ($^1O_2$) by photosensitization from brominated carbon nanodots (pH = 3, $\lambda_{exposure}$ = 365 nm, ~0.5 J•cm^{-2}) compared to control conditions. Values are reported for *A)* oxygen, *B)* air, and *C)* argon purged systems. Values are the average of a minimum of three trials for each condition, with error from standard deviation reported. **1.00 > p > 0.10, **p = 0.10, ***p = 0.05, ****p ≤ 0.01.*

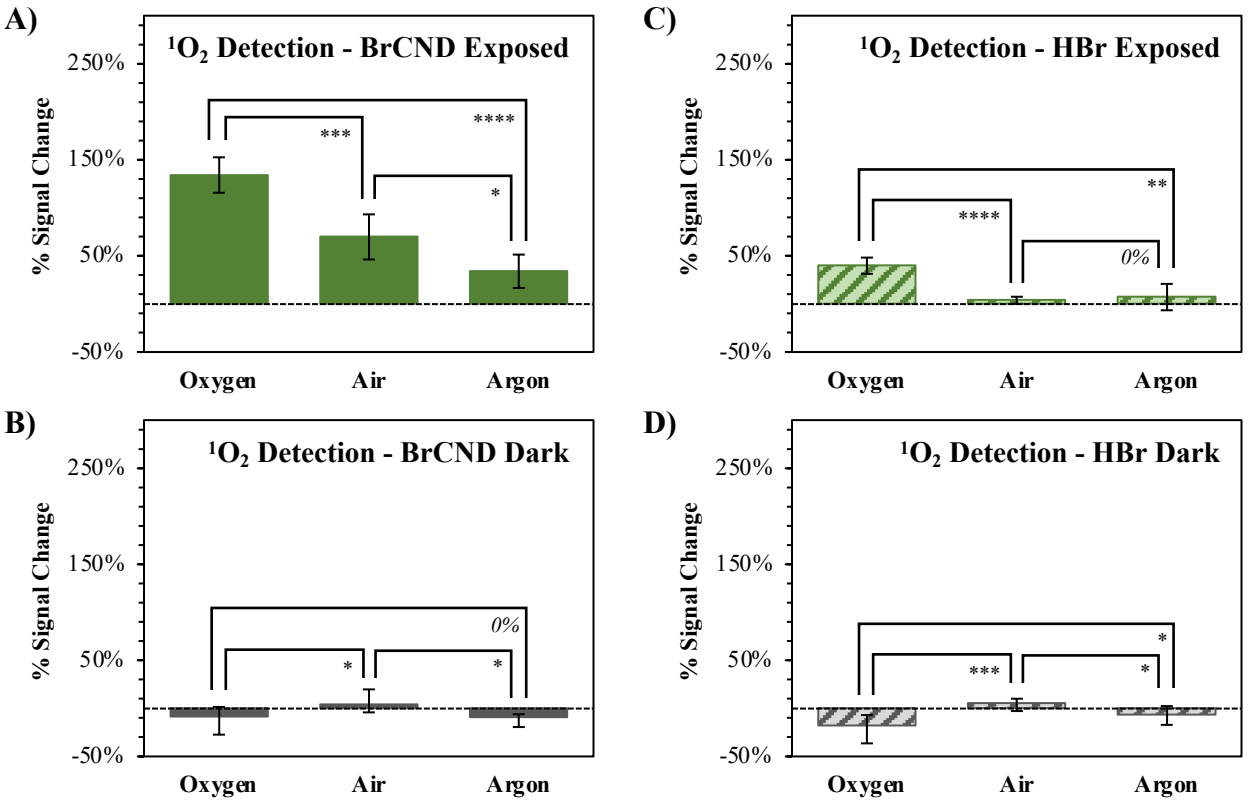

Figure S4. Statistical analysis of percent signal change values determined for singlet oxygen generation ($^1O_2$) by photosensitization from *A)* UV-exposed brominated carbon nanodots ("BrCND," pH = 3, $\lambda_{exposure}$ = 365 nm, ~0.5 J•cm^{-2}) compared to control conditions including *B*) unexposed (dark) BrCND, *C)* exposed hydrobromic acid ("HBr") solution, and *D)* unexposed HBr. Values are the average of a minimum of three trials for each condition, with error from standard deviation reported. **1.00 < p ≤ 0.20, **p = 0.10, ***p = 0.05, ****p ≤ 0.02.*

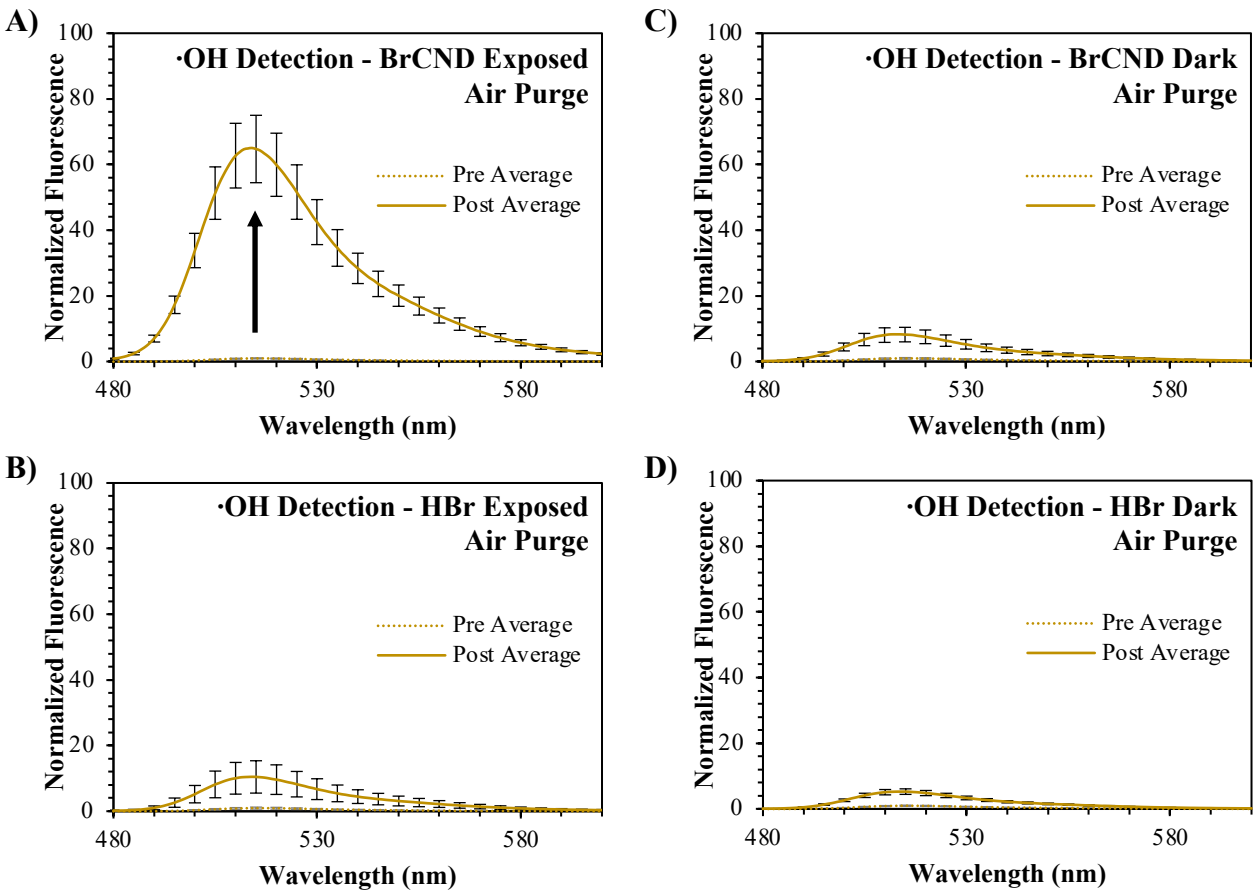

Figure S5. Normalized fluorescence spectra of Hydrophenyl Fluorescein ("HPF," $\lambda_{excitation}$ = 473 nm) before ("pre," maximum intensity = 1) and after ("post") exposure with brominated carbon nanodots ("BrCND," pH = 3.0, $\lambda_{exposure}$ = 365 nm, 1 J•cm^{-2}) under air-purged conditions. Fluorescence spectra are reported for HPF UV-exposed with *A)* BrCND and *B)* hydrobromic acid ("HBr," pH = 3.0) control, and under dark conditions (no exposure) for *C)* BrCND and *D)* HBr control solution. Reported spectra are the average of a minimum of three independent trials.

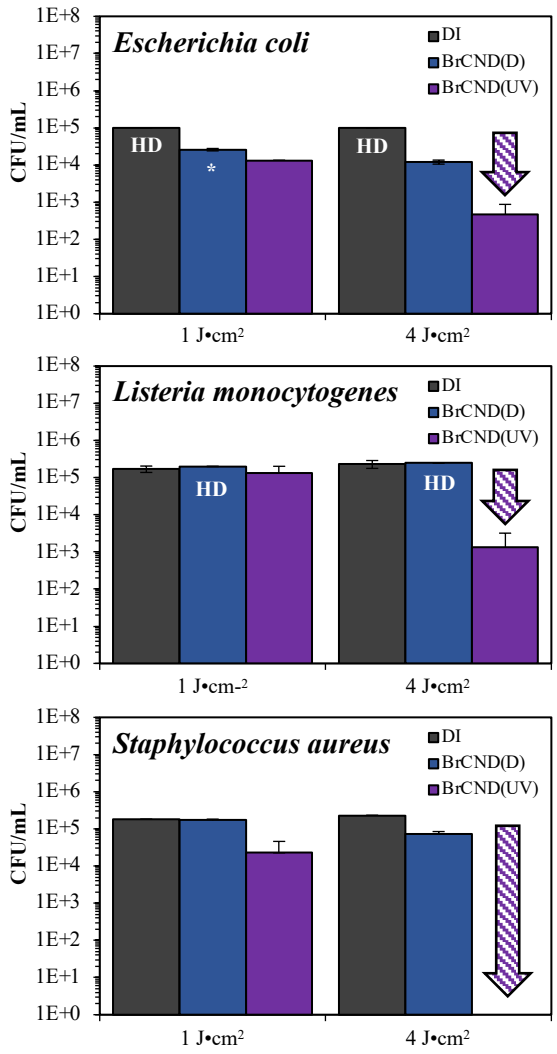

Figure S6. Results of bacterial growth inhibition from photosensitization of brominated carbon nanodots (pH 3.2 ± 0.2, $\lambda_{exposure}$ = 365 nm, 3 mW), presented in the main text figure 4. Strains tested include *A) Escherichia coli, B) Listeria monocytogenes,* and *C) Staphylococcus aureus.* Labels correspond accordingly: "DI" – deionized water only, pH 5.5; "BrCND(D)" – brominated carbon nanodots adjusted to pH 3.2, no UV exposure; "BrCND(UV)" – brominated carbon nanodots adjusted to pH 3.2 with exposure. Note: concentrations of BrCND are variable between bacterial strains, but not between energy densities. Colony growth too dense for adequate counting is indicated as "HD" and is estimated by the maximum colony count obtained in n = 3 trials; high density estimates are indicated by "*". Error is from standard deviation of n = 3 trials.

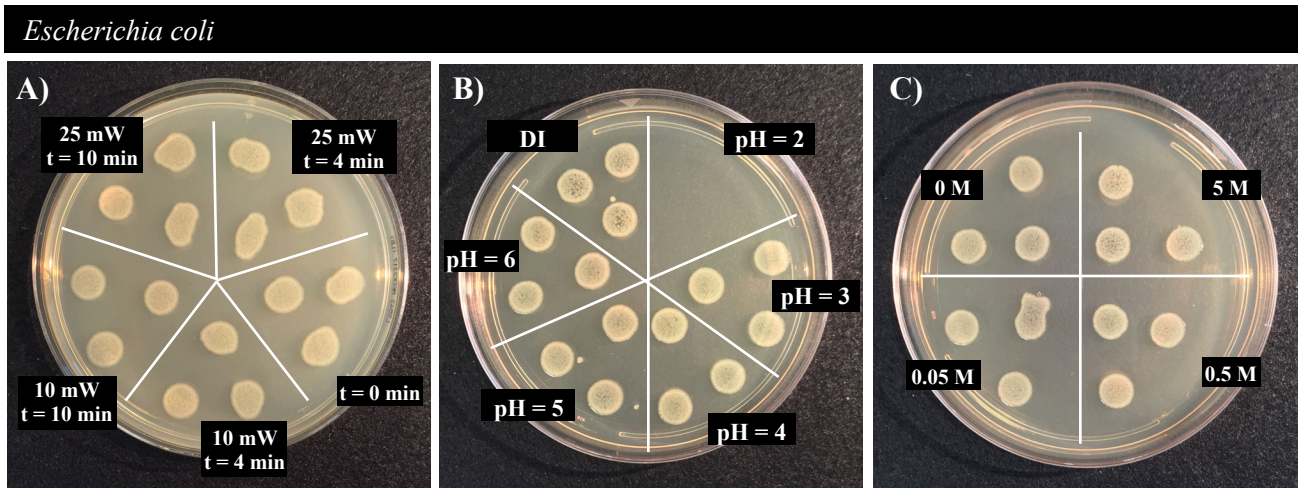

Figure S7. *Escherichia coli* control experiments for inactivation by brominated carbon nanodot photosensitization. *A)* Effects of UV ($\lambda_{exposure}$ = 365 nm) exposure on bacteria alone at 10- and 25-mW exposure powers (power measured at 400 nm) for 4- and 10-minute exposure intervals. *B)* Effects of exposure solution pH on bacteria alone for a pH range of 2 to 6. *C)* Effects of bromide ion concentration in exposure solution for bacteria alone for concentrations ranging from 0- to 5-M.

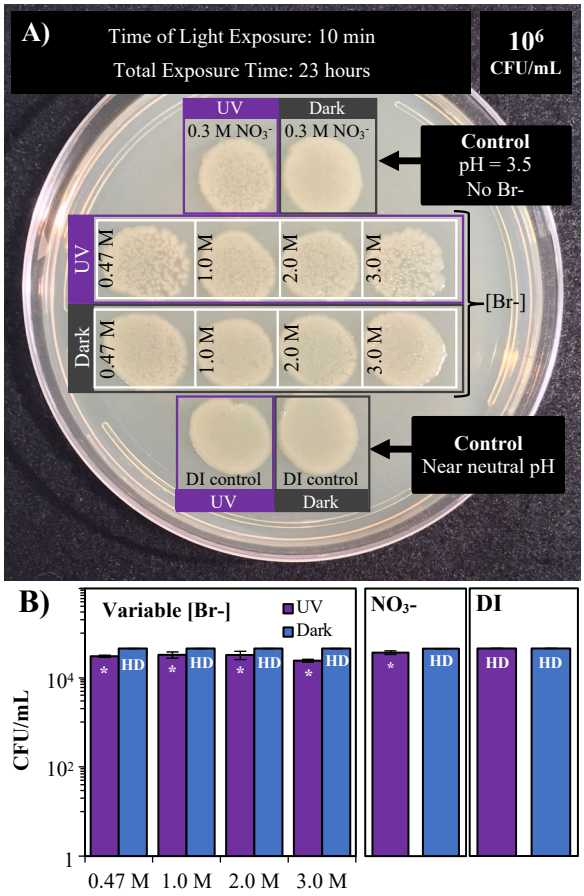

Figure S8. *Escherichia coli* growth dependence on variable concentrations of bromide ion at pH = 3.5. *A)* Photograph of *E. coli* growth on LB agar after 10 minute exposure under various conditions followed by incubation. *B)* Colony counts for each sample shown in (A). Error is from counts by 3x individuals to reduce bias in manual counting. Colony growth too dense for adequate counting is indicated as "HD" and is estimated by the maximum colony count obtained in n = 3 trials; high density estimates are indicated by "*".

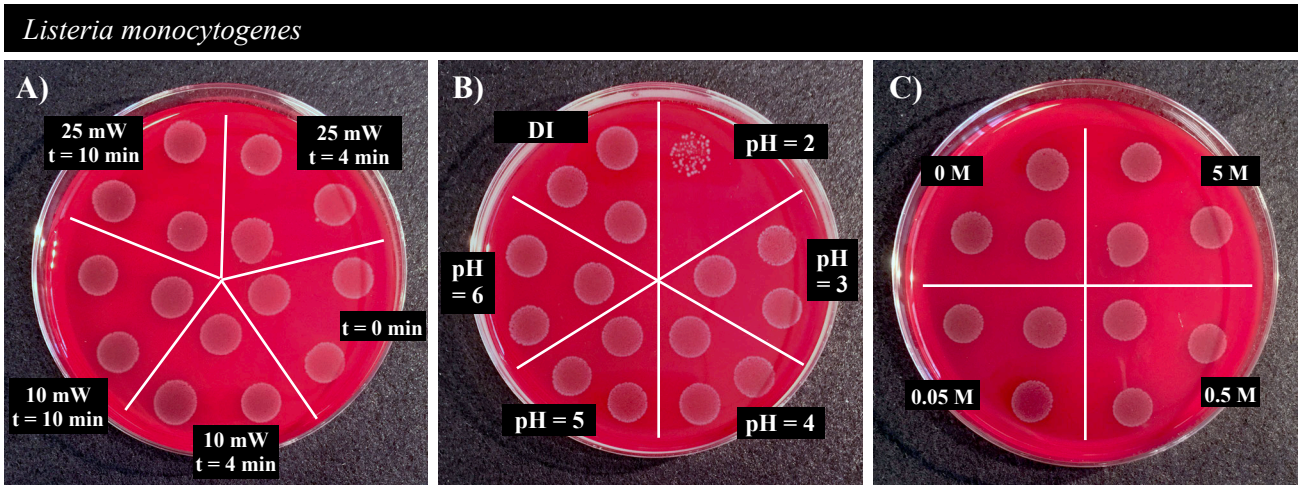

Figure S9. *Listeria monocytogenes* control experiments for inactivation by brominated carbon nanodot photosensitization. *A)* Effects of UV ($\lambda_{exposure}$ = 365 nm) exposure on bacteria alone at 10- and 25-mW exposure powers (power measured at 400 nm) for 4- and 10-minute exposure intervals. *B)* Effects of exposure solution pH on bacteria alone for a pH range of 2 to 6. *C)* Effects of bromide ion concentration in exposure solution for bacteria alone for concentrations ranging from 0- to 5-M.

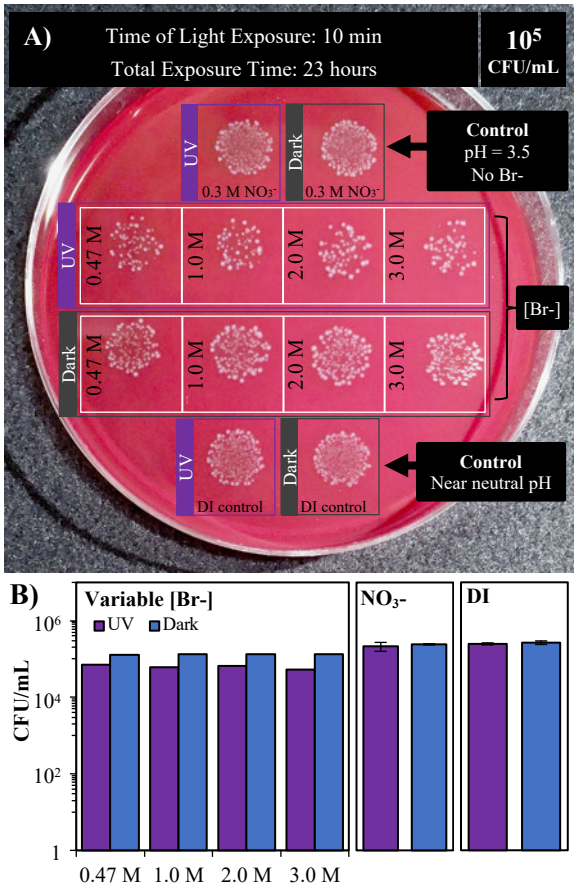

Figure S10. *Listeria monocytogenes* growth dependence on variable concentrations of bromide ion at pH = 3.5. *A)* Photograph of *L. monocytogenes* growth after 10-minute exposure under various conditions followed by incubation. *B)* Colony counts for each sample shown in (A). Error is from 3x repeated counts to reduce bias in manual counting.

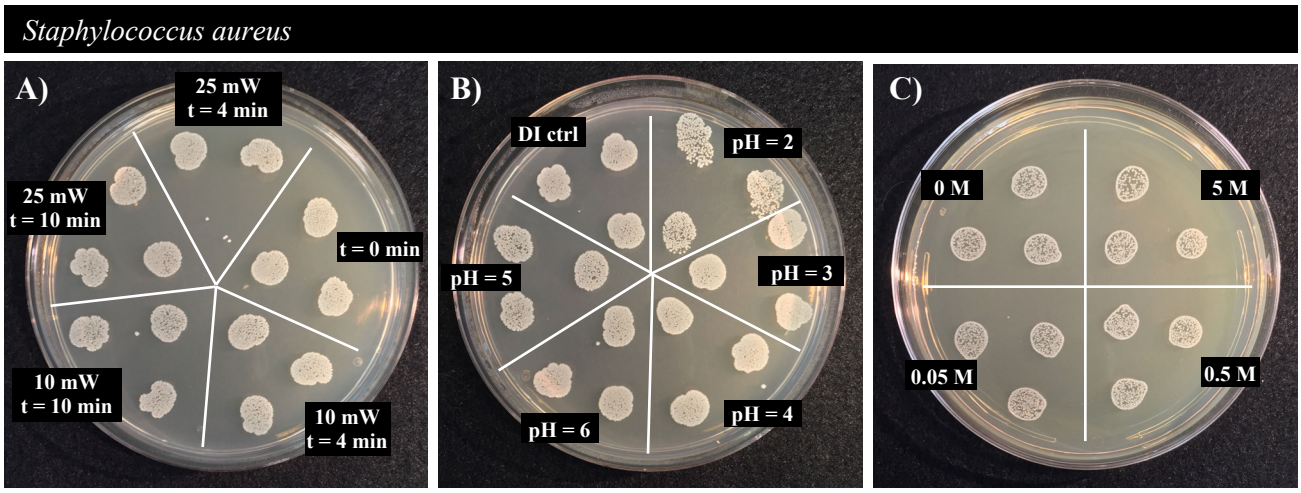

Figure S11. *Staphylococcus aureus* growth control experiments for inactivation by brominated carbon nanodot photosensitization. *A)* Effects of UV ($\lambda_{exposure}$ = 365 nm) exposure on bacteria alone at 10- and 25-mW exposure powers (power measured at 400 nm) for 4- and 10-minute exposure intervals. *B)* Effects of exposure solution pH on bacteria alone for a pH range of 2 to 6. *C)* Effects of bromide ion concentration in exposure solution for bacteria alone for concentrations ranging from 0- to 5-M.

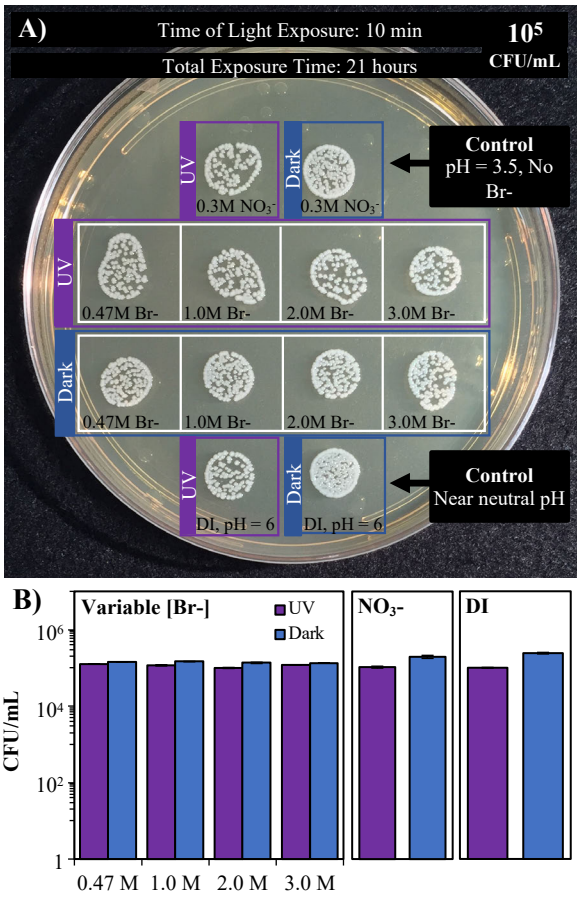

Figure S12. *Staphylococcus aureus* growth dependence on variable concentrations of bromide ion at pH = 3.5. *A)* Photograph of *S. aureus* growth on LB agar after 10 minute exposure under various conditions followed by incubation. *B)* Colony counts for each sample shown in (A). Error is from counts by 3x individuals to reduce bias in manual counting.

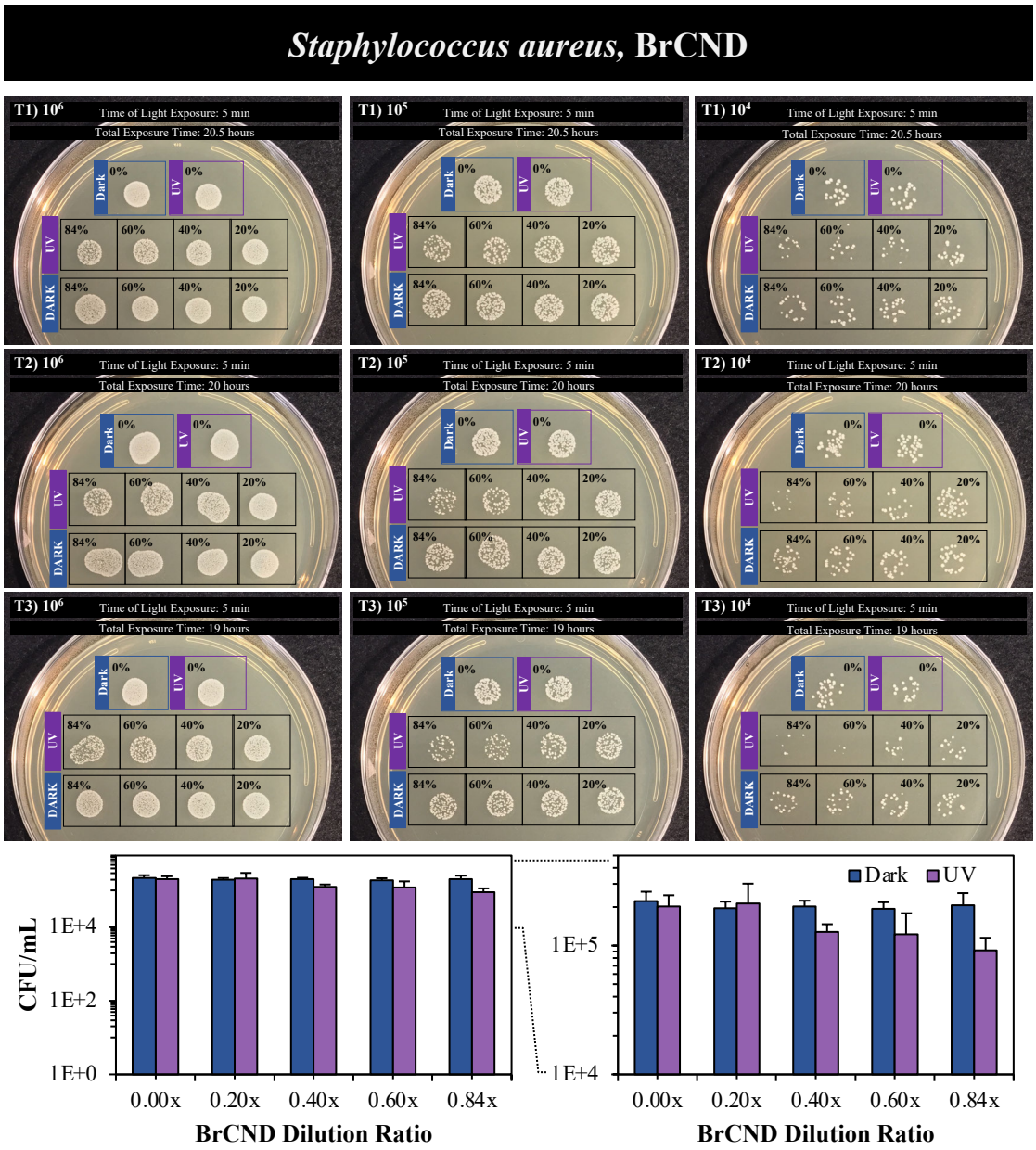

Figure S13. Real-color photographs and corresponding antibacterial activity of *Staphylococcus aureus* exposed to bromine dot ("BrCND") solutions of varying concentrations (dilution ratios) under either no-light ("dark") or UV-exposed ("UV," $\lambda_{exposure}$ = 365 nm, 3.0 ± 0.1 mW, 2 J•cm^{-2}) conditions. The data here is all the experimental data for the n = 3 trials ("T") used in further analysis, presented in figures 6 and 7 of the main text. *Left* – 10^6 CFU/mL sample; *Middle* – first log dilution, 10^5 CFU/mL; *Right* – second log dilution, 10^4 CFU/mL.

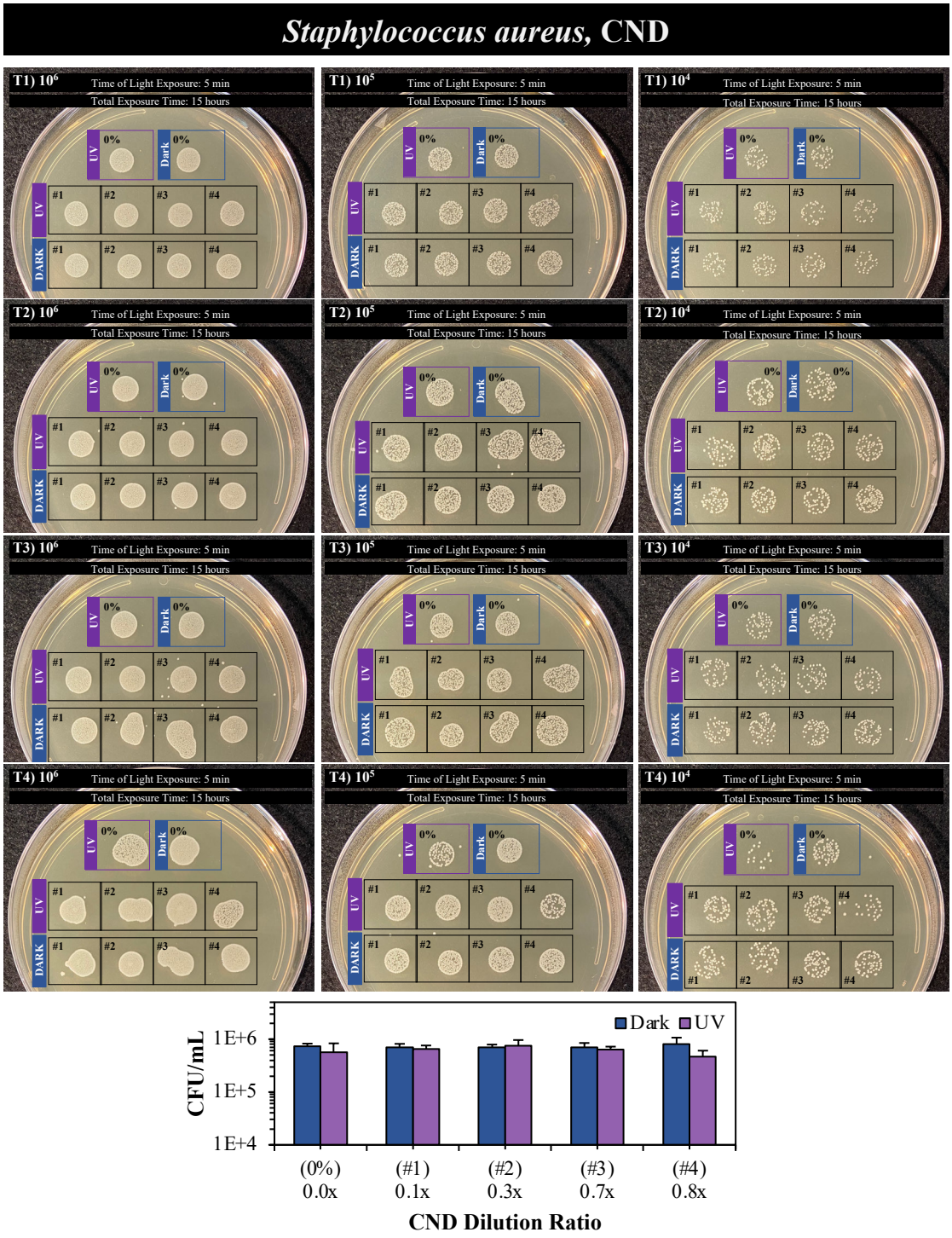

Figure S14. Real-color photographs and corresponding antibacterial activity of *Staphylococcus aureus* exposed to carbon dot ("CND") solutions of varying concentrations (dilution ratios) under either no-light ("dark") or UV-exposed ("UV," $\lambda_{exposure}$ = 365 nm, 3.0 ± 0.1 mW, 2 J•cm^{-2}) conditions. The data here is all the experimental data for the n = 4 trials ("T") used in further analysis, presented in figure 7 of the main text. *Left* – 10^6 CFU/mL sample; *Middle* – first log dilution, 10^5 CFU/mL; *Right* – second log dilution, 10^4 CFU/mL.

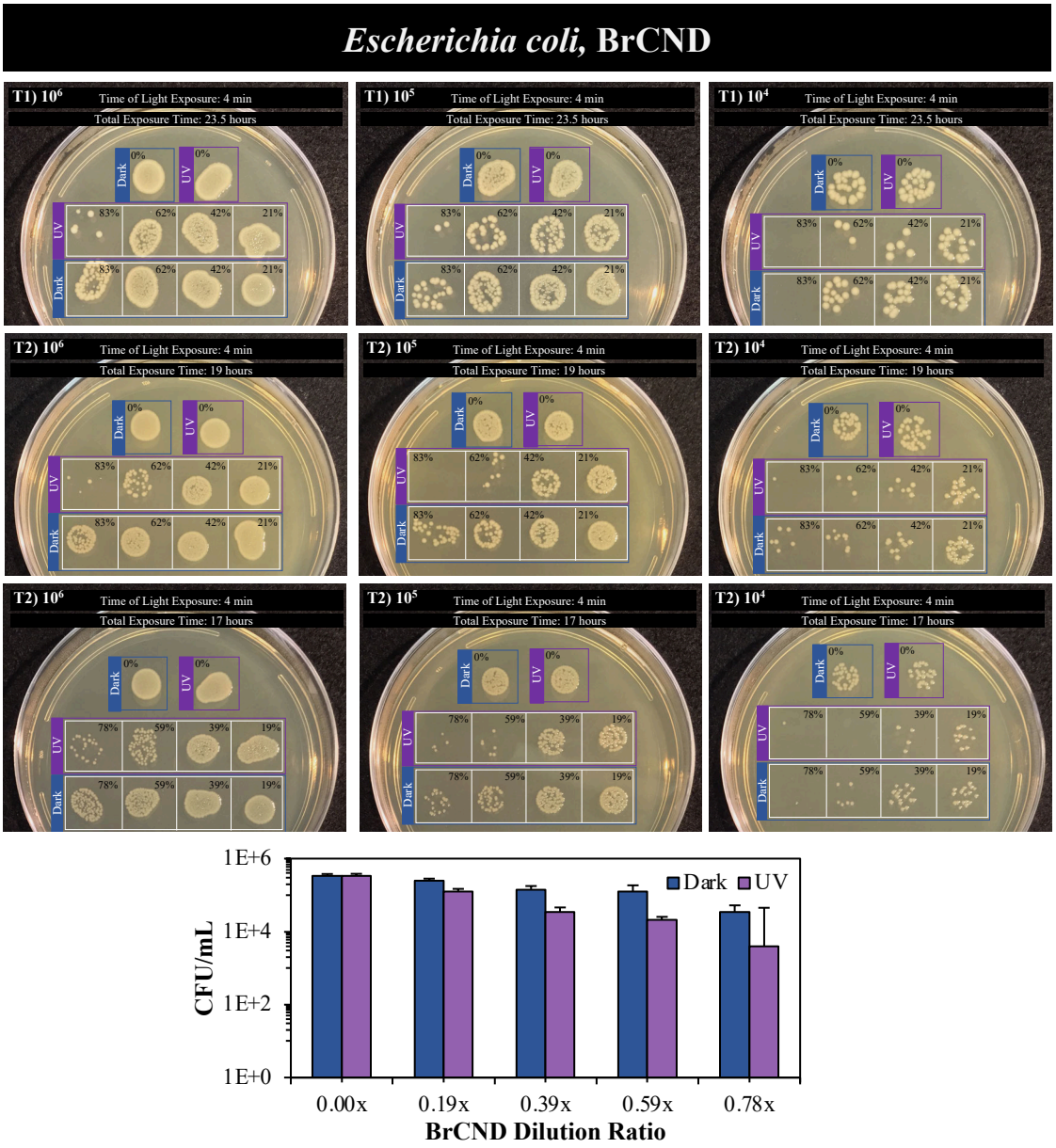

Figure S15. Real-color photographs and corresponding antibacterial activity of *Escherichia coli* exposed to bromine dot ("BrCND") solutions of varying concentrations (dilution ratios) under either no-light ("dark") or UV-exposed ("UV," $\lambda_{exposure}$ = 365 nm, 3.0 ± 0.2 mW, 1 J•cm^{-2}) conditions. The data here is all the experimental data for the n = 3 trials ("T") used in further analysis, presented in figures 7 and 8 of the main text, and ESI figure S18. *Left* – 10^6 CFU/mL sample; *Middle* – first log dilution, 10^5 CFU/mL; *Right* – second log dilution, 10^4 CFU/mL.

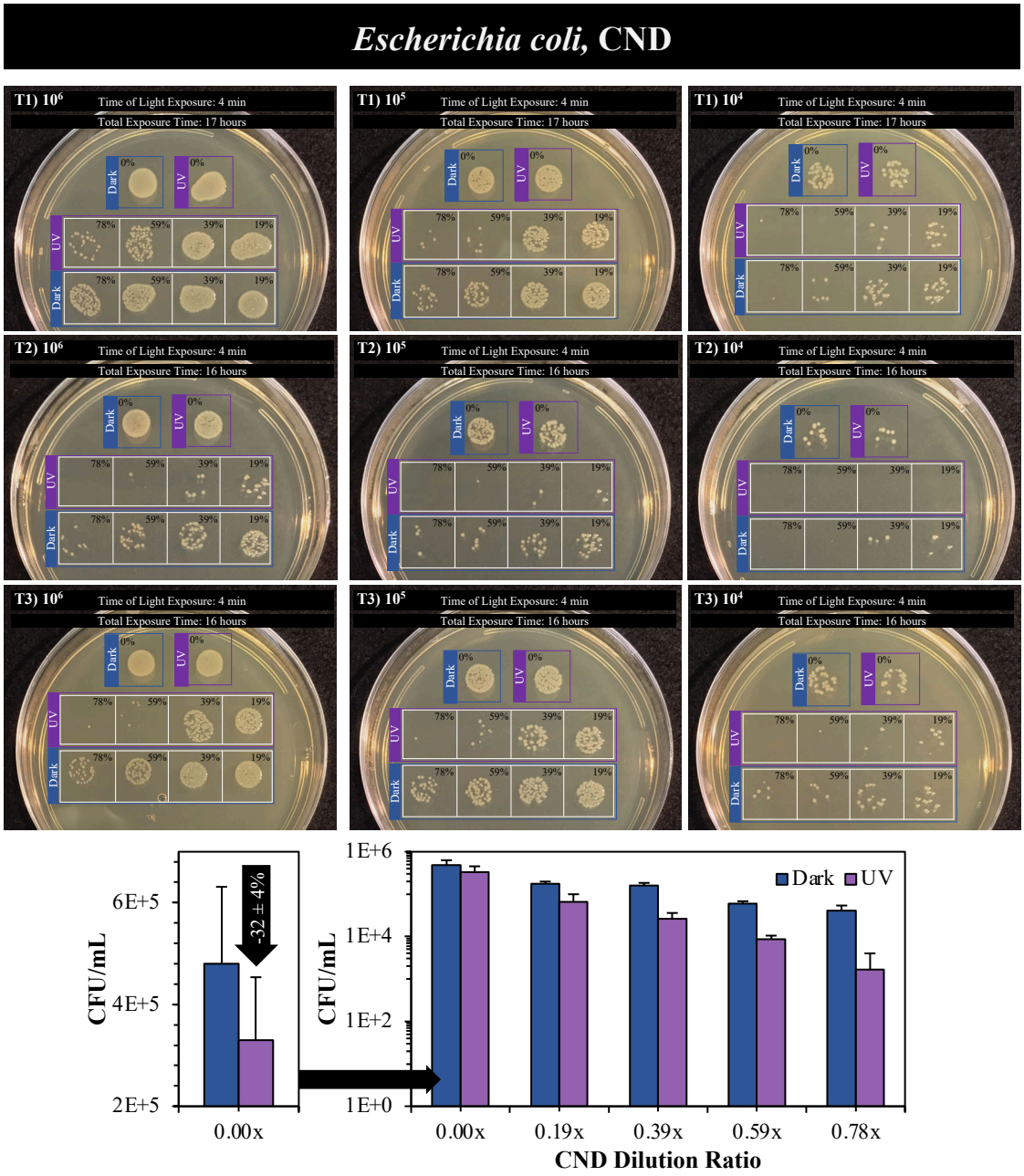

Figure S16. Real-color photographs and corresponding antibacterial activity of *Escherichia coli* exposed to carbon dot ("CND") solutions of varying concentrations (dilution ratios) under either no-light ("dark") or UV-exposed ("UV," $\lambda_{exposure}$ = 365 nm, 3.0 ± 0.2 mW, 1 J•cm^{-2}) conditions. The data here is all the experimental data for the n = 3 trials ("T") used in further analysis, presented in figure 7 of the main text. *Left* – 10^6 CFU/mL sample; *Middle* – first log dilution, 10^5 CFU/mL; *Right* – se8ond log dilution, 10^4 CFU/mL.

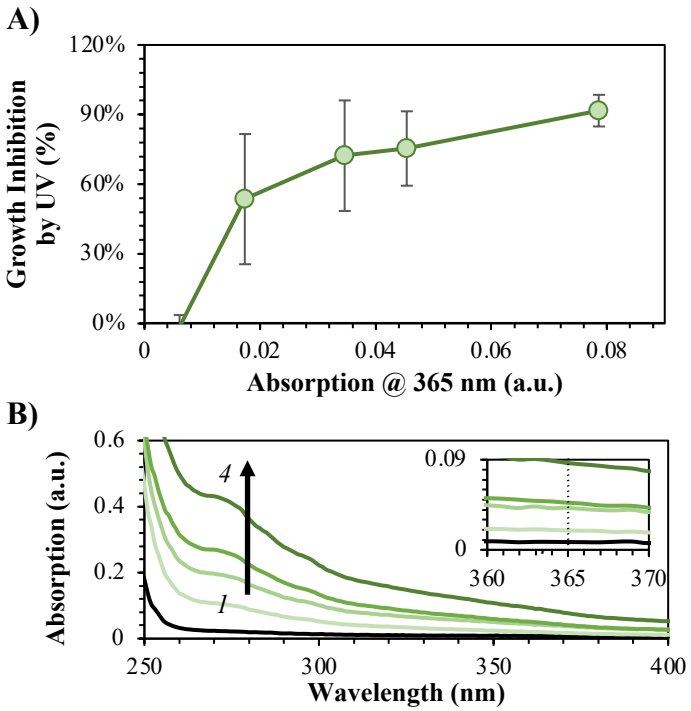

Figure S17. Viability of *Escherichia coli* after 4-minute exposure to brominated carbon nanodot ("BrCND") solutions of varying concentrations. Bacterial samples were both kept in dark (no light) and photosensitization ($\lambda_{exposure}$ = 365 nm or "UV", 3.0 ± 0.2 mW, 1 J•cm^{-2}) conditions at a pH of 3.0. *A)* Growth inhibition due to UV photosensitization for each solution absorption at the photosensitization wavelength. Error is from the standard deviation of n = 3 trials. *B)* Absorption spectra of each BrCND solution (1-4, Fig. 7-8). Black line is the absorption of the control solution. **Inset**. Magnified absorption window at the photosensitization wavelength.

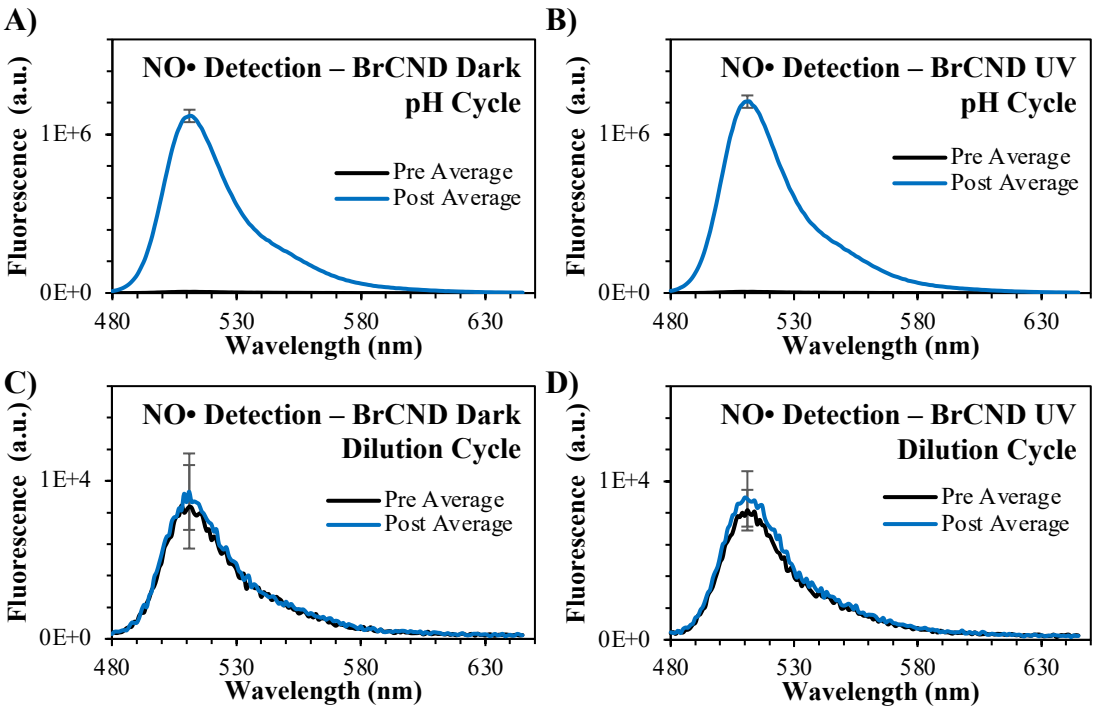

Figure S18. Fluorescence spectra of Diaminofluorescein-FM ("DAF-FM," $\lambda_{excitation}$ = 473 nm) before ("pre") and after ("post") exposure with brominated carbon nanodots ("BrCND," pH = 3.0, $\lambda_{exposure}$ = 365 nm, 0.56 ± 0.04 mW, 0.1 J•cm^{-2}). Fluorescence spectra are reported for DAF-FM pH cycled under *A)* dark and *B)* UV-exposed conditions and dilution cycled (pH 12-12.5) for *C)* dark and *D)* UV-exposed conditions. Reported spectra are the average of n = 3 independent trials.